

Numerical Study on the Ballistic Performance of Twaron®/Epoxy Laminated Composite Plates Manufactured by Vacuum Assisted Resin Infusion Moulding Against 9 mm Bullet Threat

Tayfur Kerem DEMİRCİOĞLU*¹ ORCID 0000-0002-0518-0739
Fatih BALIKOĞLU¹ ORCID 0000-0003-3836-5569

¹Mechanical Engineering Department, Engineering Faculty, Balıkesir University, Balıkesir

Geliş tarihi: 15.03.2022 Kabul tarihi: 30.06.2022

Atıf şekli/ How to cite: DEMİRCİOĞLU, T.K., BALIKOĞLU, F., (2022). Numerical Study on the Ballistic Performance of Twaron®/Epoxy Laminated Composite Plates Manufactured by Vacuum Assisted Resin Infusion Moulding Against 9 mm Bullet Threat. Çukurova Üniversitesi, Mühendislik Fakültesi Dergisi, 37(2), 483-497.

Abstract

This article presents the experiments on the ballistic effect of plates formed by stacked Twaron® fabrics between 10 and 16 layer numbers impregnated with epoxy resin by vacuum infusion method and the results of Autodyn-2D® simulations using an axisymmetric model. The ballistic impact resistance of the panels produced was determined according to the NIJ-STD-0108.01 standard. All panels were tested against 9 mm FMJ bullets at an average velocity of 390 m/s with the MP5 gun for armour application. The interaction of the plates with the bullet, the post-shot damage photographs, residual velocities of the bullet were compared with Autodyn-2D® simulations. Parametric study was performed in the analysis to determine the optimum bullet velocity, layer thickness and tensile failure strain. It was observed that the data obtained from the simulations were consistent with the experiments.

Keywords: Twaron®/epoxy composite, Ballistic test, VARIM

Vakum Destekli Reçine İnfüzyon Kalıplama ile Üretilmiş Twaron®/Epoksi Lamine Kompozit Plakaların 9 mm Mermi Tehdidine Karşı Balistik Performansı Üzerine Sayısal Çalışma

Öz

Bu makale, vakum infüzyon yöntemiyle epoksi reçine emdirilen 10 ile 16 katman sayıları arasındaki istiflenmiş Twaron® kumaşların oluşturduğu plakaların balistik etkisi üzerine yapılan deneyleri ve eksenel simetrik modellenen Autodyn-2D® simülasyonlarından elde edilen sonuçları sunmaktadır. Üretilen panellerin balistik darbe dayanımı NIJ-STD-0108.01 standardına göre belirlenmiştir. Tüm paneller, zırh uygulaması için MP5 silahı ile ortalama 390 m/s hızına sahip 9 mm FMJ mermilere karşı test edilmiştir. Plakaların mermi ile etkileşimi, atış sonrası hasar fotoğrafları, kurşunun artık hızları, Autodyn-2D® simülasyonları ile karşılaştırılmıştır. Optimum mermi hızı, tabaka kalınlığı ve çekme hasarı

*Sorumlu yazar (Corresponding author): Tayfur Kerem DEMİRCİOĞLU, tkerem@balikesir.edu.tr

gerinim deęerini belirlemek için analizde parametrik alıřma yapılmıřtır. Simülasyondan elde edilen verilerin deneylerle tutarlı olduęu görölmüřtür.

Anahtar Kelimeler: Twaron®/epoksi kompozit, Balistik test, VARIM

1. INTRODUCTION

Composite structures are subjected to a variety of loading conditions throughout their service lives. A critical requirement for the effective use of composites as protective structures is their resistance to foreign object impact events. For this, high strength, stiffness, and toughness properties may be required for fibre reinforced composite materials to withstand such impact loads [1]. Impact events can occur at low (1-10 m/s), moderate (10-50 m/s), ballistic (50-1000 m/s), and hyper (2-5 km/s) speeds [2]. The reason for this classification is that with a change in impact velocity, there is a considerable difference in the amount of energy transfer, energy loss, and damage progression mechanisms between the target and the projectile. Light armour applications are critical to ensuring the protection of personnel and equipment against high-speed bullet penetration. As a result, it's crucial to analyse the penetration and perforation processes of a projectile/object into composite materials at ballistic speeds. The main energy absorption mechanisms during ballistic impact are as follows; the formation of the moving cone on the back of the target, the projectile cutting the target, the tensile damage of the primary yarns and elastic deformation of the secondary yarns, the matrix cracking and delamination failures, the friction between the projectile and the target during penetration. The mechanical characteristics of the fibres and matrix, the stacking sequence, the physical properties of the bullet/object and laminates, bullet mass, shape, and velocity, and layer thickness all influence the ballistic performance of laminated composites [3].

There are three approaches to dealing with problems involving the release of large amounts of energy in a very short time in ballistic impacts: most of the work is experimental and therefore can be very costly, as the problems are non-linear and

require knowledge of material behaviour at high loading rates. Analytical approaches are possible if the geometries are relatively simple and the loading, boundary, and initial conditions can be defined. The explicit methods are much more general in scope and eliminate all geometry-related difficulties and use very small-time steps for results [4]. The material models employed for these methods, on the other hand, need the use of a large number of material properties and model variables [5].

In the literature, there are many numerical studies focused on the ballistic performance of textile composite materials [6-17]. For a constant thickness hybrid composite armour containing glass (GF), carbon (CF) and Kevlar® (KF) fibres, an axisymmetric model was designed in ANSYS/Autodyn-2D® and it was observed that the stacking order of the layers and the STAGNAG-2920 fragment simulating bullet geometry had a significant effect on the ballistic performance. Authors reported that the KF layer on the rear, the GF layer on the outside, and the CF layer on the front provided superior ballistic impact protection [6]. In another study, the ballistic impact behaviour of Kevlar®/Polypropylene (PP) panels was investigated through hydrocode simulations conducted with Ansys Autodyn-2D® software. The numerical model was validated by evaluating the ballistic impact performance of Kevlar/PP composites when impacted by STANAG-2920 fragment simulating projectiles [7]. In addition, simulations were carried out for 9 mm parabellum bullets modelled by the Smooth Particle Hydrodynamics method (SPH) and 20 layers of Kevlar plates coded with Lagrange grid in Autodyn® program. Gauge points were determined for the velocity of the projectile and compared with the average velocity of the projectile. Erosion (cell removal) criteria were applied due to the interruption of the simulation with very large

deformations of the grid. The authors also investigated the effect of erosion strain on the mass of the removed cells and the residual velocity of the projectile [8]. The deformation of bullets after ballistic testing was also numerically studied. Mushroom deformation as a result of the 9 mm Parabellum bullet hitting Armox 500 armour steel, as well as the length of the bullet and the depth of the hole produced by the deformed bullet were also investigated in Ansys-Autodyn-3D[®] simulations. In the 2D-axial symmetry numerical simulations, the friction coefficients between the shell and the core of the bullet were considered [9]. Numerical analysis and experimental results of the ballistic impact performances of military helmets were also examined [10,11]. The results obtained from the Autodyn-3D[®] simulations showed that the helmet made of Kevlar[®] material could stop a 9 mm full jacketed bullet with a ballistic velocity of 358 m/s. The findings of the helmet models were found to be consistent with the results of the experiments. The effects of bullet velocity, diameter, and mass on the ballistic impact behaviour of the targets were also investigated using numerical simulation in Autodyn[®] program. With the increase of the impact velocity up to the ballistic limit velocity, the contact time first increased and then decreased, so the damage mechanisms before and after the ballistic limit changed [12]. Moreover, the effect of bullet nose geometry on penetration time and residual velocity were investigated using Autodyn[®] software. It was reported that the ballistic limit velocity increased faster for the conical ended cylindrical bullet for different thickness/edge length values of the test panel compared to the blunt-ended counterpart [13]. In the analysis of the ballistic behaviour of composite armour designs consisting of three different materials, fibre-cement, Kevlar fabric and steel, against the 9 mm FMJ bullet, Autodyn-3D[®] simulation results were found to be compatible with the experimental results [14]. In order to simulate the Twaron[®] CT709 ballistic fabric against the threat of 9 mm FMJ Parabellum projectile, importing the CAD model drawing of the fabric to Autodyn[®] software was applied in the literature. For ballistic panels made of 16 layers of Twaron[®] CT709 fabric,

decrease of projectiles velocity and projectiles shortening values were obtained [15]. The ballistic performance of Twaron[®] CT709 plain woven fabrics was also investigated in the ABAQUS[®]/Explicit program using a three-dimensional fabric model. The authors conducted a parametric study to analyse the effects of various parameters such as impact velocity, inter-fibre friction and fabric layer count on the impact behaviour of fabrics. This parametric study provided the optimal number of fabric layers and optimized inter-yarn friction level to be determined to accomplish maximum energy absorption at the given impact velocities [16]. Using the LS-Dyna[®] software, a finite element analysis of the interaction process of the Para-aramid Twaron[®] multilayer body armour and the human body with the 9 mm Parabellum bullet with a velocity of 366±10 m/s was conducted, taking into consideration the real geometries of the objects. The authors applied numerical modelling to study how to optimize the energy absorbed by the human body by varying the number of layers and material of the body armour. Furthermore, the energy absorbed by the human body was estimated using simulation responses during a non-perforated impact tests [17].

To the authors' knowledge, no research studies have been conducted in the fields of ballistics on the results of two-dimensional axisymmetric numerical modelling of Twaron[®] CT709/epoxy plates in Autodyn[®] software, which is expected to fill the gap in the literature. In addition, Twaron[®] CT709/epoxy plates were also manufactured for experimental tests using a vacuum assisted resin infusion moulding method, with the results expected to provide valuable data for the marine industry. In this proposed study, to meet the Level 2-2A protection level according to NIJ-STD-0108.01 standards, a 9 mm round nose full metal jacket bullet (FMJ RN) with an 8g (123gr) brass-plated lead core (muzzle velocity 390 m/s, shot from 5 meters) was used in the experimental study. The ballistic behaviour of Twaron[®]-CT709[®] (1.45g/cm³) aramid fabric/epoxy plates produced by vacuum assisted resin infusion moulding and the deformation of the bullet were numerically

investigated with Autodyn-2D® software and verified with experimental results.

2. MATERIAL AND METHOD

2.1. Test Samples and Production

Aramid fabrics were cut to 325×325 mm dimensions for ballistic tests. The number of layers was determined as 10, 12, 14, 16. Plain woven Twaron® CT709® (1.45g/cm³) brand para-aramid fibres with 200 g/m² unit area weight, infusion type

epoxy resin was used as matrix [18, 19]. After the liquid resin-hardener mixture was vacuumed into the flat mould under -700 mm Hg pressure, the laminate was cured in a vacuum bag for 24 hours. Stacked aramid layers were produced by the VARIM (vacuum assisted resin infusion moulding) method (Figure 1). The matrix material was Hexion L160 epoxy resin, which can be cured at room temperature and has a specific hardener (Hexion H160). According to the manufacturer, the ratio of resin to hardener by weight was applied as 4:1 [20].

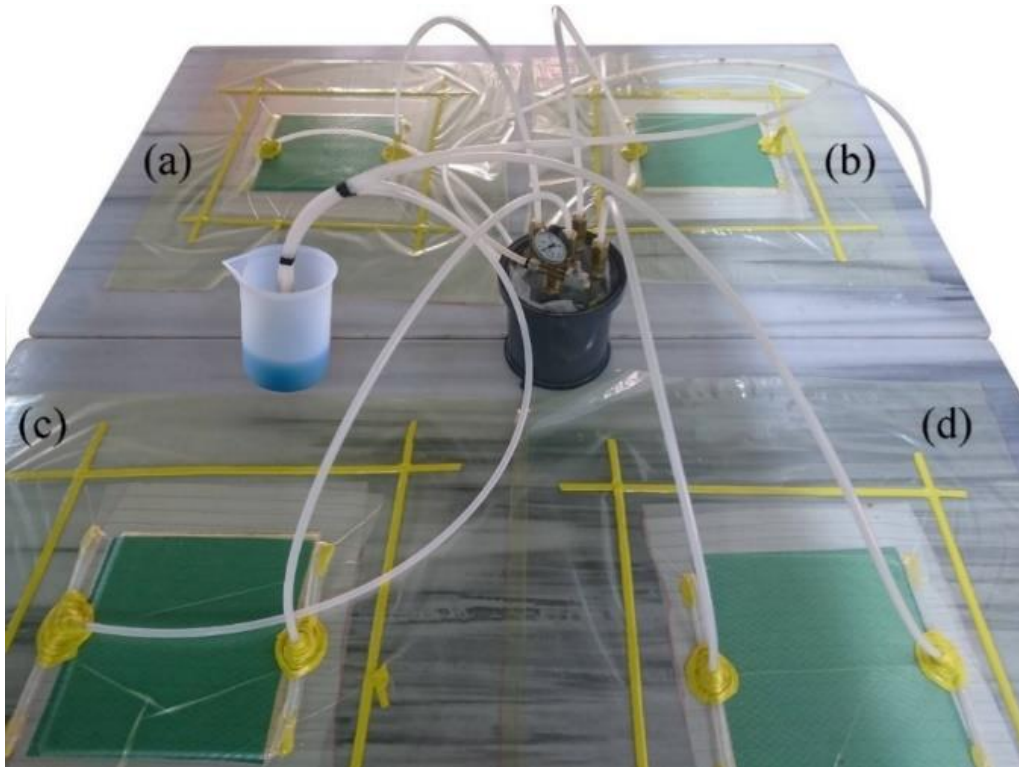


Figure 1. Production of aramid plates by VARIM method. (a) 10-layer, (b) 12-layer, (c) 14-layer, (d) 16-layer ballistic plates

2.2. Ballistic Tests

Ballistic tests were carried out in the polygon field of ZSR Patlayıcı Inc. The tests were conducted with an MP5 gun and a 9 mm, 8 gr (123g) FMJ RN (Full Metal Jacket Round Nose) bullet. The experiments were performed in compliance with the NIJ-STD-0108.01 requirements at the

protection level 2-2A [21]. Chronographs were attached to tripods and placed at a distance of 2.5 meters in front and behind the plates to measure the barrel and exit velocities. The distance between the barrel and the sample was determined as 5 meters (Figure 2). The samples were fixed by placing the plate holder on the test setup frame and tightening the eight bolts on it with a constant

torque of 40 Nm. The angle between the flight line of the bullet and the front face of the sample was set as perpendicular as possible. After the MP5 was fixed and its horizontality checked a maximum of

five shots were fired at each plate (Figure 3). The mean/difference/standard deviation values were calculated by measuring the initial-barrel and residual-exit velocities of the bullets.

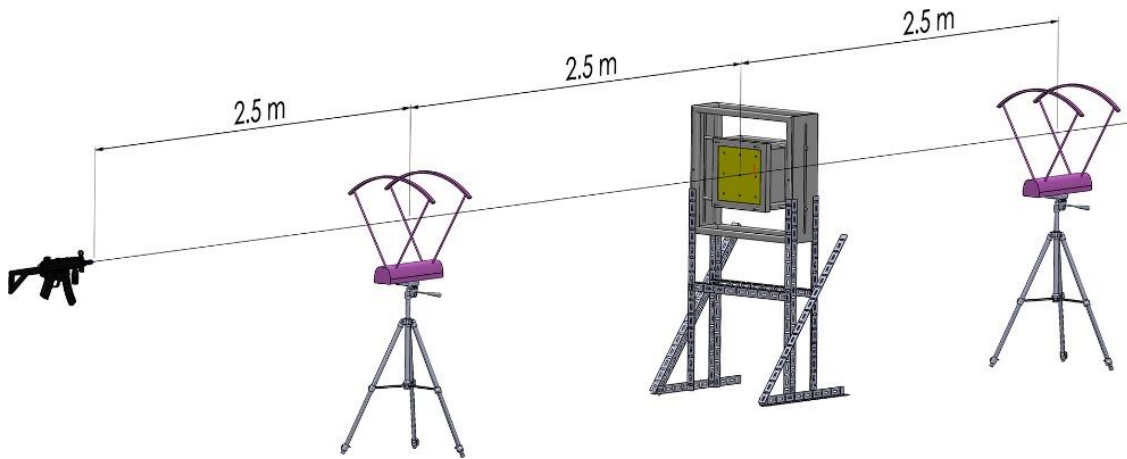


Figure 2. Ballistic test set-up in accordance with NIJ-STD-0108.01 standard



Figure 3. Testing with MP5 gun 9 mm FMJ bullet at the shooting range

A new model was created in accordance with the dimensions of the Ø 9 mm FMJ bullet (total length of 15 mm, brass material thickness of 0.25 mm, lead material radius of 4.25 mm) by adding predefined box, quad, ogive geometric shapes in Autodyn-2D program. Composed of an inner core (lead 7.2818 g) and a cartridge/outer shell (brass 0.74473 g), the total mass of the bullet was set at approximately 8 g. Twaron®/epoxy plate and bullet geometry were divided into quadrilateral elements by using the structured mesh type. In the lead core, the smallest quadrilateral element mesh size was set at 0.2 mm, and for the Twaron®/epoxy ballistic plate, it was adjusted between approximately 0.24 and 0.26 mm. The number of elements and nodes for bullet and plate were given in Table 1. A more precise structure close to the smallest element size of the bullet was obtained by keeping the mesh element size constant between 0.24-0.26 mm in the X (along thickness) and Y (along length) direction (50 grid/cell) in the bullet impact zone of the plate where the deformation was higher. The length of the plate is modelled as 150 mm axisymmetric and divided into a total of 150 elements with 50 cells fixed and the rest increasing dimensions (Figure 4). The effect of the

mesh element number on the convergence of analysis results was also examined and seen that minimum mesh size (between 0.10-0.13 mm) no longer changed the residual velocity results.

Analyses were made for three different velocities (380, 390 and 400 m/s) in accordance with the standard deviation values of the initial velocity of the bullet measured from ballistic tests (Table 3). The average thickness/number of layers ratio of the plates measured in the experimental study was between 0.26-0.28 mm (Figure 5a) and the thickness of the woven Twaron® CT 709 in the handbooks and literature was 0.30 mm [8, 23, 24]. As a result, one layer thickness was modelled for three different values (0.26/0.28/0.30 mm) in the analysis. The reason for the thickness change was due to production under vacuum. Tensile failure strain (TFS) values of 0.033, 0.0345, 0.04, and 0.046 were found in the literature for CT 709 Twaron® [15-17, 19, 24, 25]. Based on these values, in addition to the 0.060 used for tensile failure strain 22 and 33 directions for Kevlar/epoxy data in Autodyn, the effect of 0.045 on the analysis results was studied.

Table 1. The number of elements and nodes for the bullet and plate

| Plate Twaron®/epoxy | (0.26 mm/layer) | | (0.28 mm/layer) | | (0.3 mm/layer) | |
|-------------------------------|------------------------|--------------|------------------------|--------------|-----------------------|--------------|
| Number of Layer | No. of Elements | No. of Nodes | No. of Elements | No. of Nodes | No. of Elements | No. of Nodes |
| 10 | 1500 | 1661 | 1650 | 1812 | 1800 | 1963 |
| 12 | 1800 | 1963 | 2100 | 2265 | 2250 | 2416 |
| 14 | 2100 | 2265 | 2400 | 2567 | 2550 | 3000 |
| 16 | 2400 | 2567 | 2700 | 2869 | 2718 | 3171 |
| Bullet | | | | | | |
| Lead | 533 | 678 | 533 | 678 | 533 | 678 |
| Cartridge Brass | 62 | 132 | 62 | 132 | 62 | 132 |

The velocity of the bullet modelled to impact the plate face perpendicularly from the centre point was given in the X direction. The common nodes of lead and brass materials were joined. A fix boundary condition of zero velocity in the X and Y directions (clamping) was imposed to the nodes with farthest distance from the symmetry axis of Twaron®/epoxy material model. The Twaron®

plate geometry is modelled on a macro scale as a (whole) non-layered structure.

The contact, sliding and separation between the bullet and the Twaron®/epoxy plate were defined using the gap interaction logic. Each surface segment was surrounded by a contact detection zone in the gap interaction logic. The gap size was

the radius of this detection zone. The node was repelled by a force proportional to the depth of its penetration when entering the detection zone of a surface segment [10]. A gap size of 0.013230 mm between the bullet and the plate was defined by the gap interaction logic.

Steinberg Guinan and Johnson-Cook strength models was used for lead and brass material, respectively and both the bullet and the target were represented by Lagrange solver. Orthotropic equation of state (EOS) was used in Twaron®/epoxy plate, shock state equation was chosen in lead and brass materials. Lead and Cartridge Brass material properties were available in the material library of Autodyn program [26]. Material properties for Twaron®/epoxy was found in the literature [10-13]. “1” indicates the material thickness direction (X), “2” indicates the fibre direction (Y), and “3” indicates the perpendicular direction to the fibre in Autodyn-2D orthotropic composite modelling.

In this simulation, material constants for Kevlar 129 were used to estimate the ballistic impact of a Twaron®/epoxy plates (Table 2). It was assumed that the difference in material properties was not

adversely affect the simulation. [10-13]. Two companies have generally pursued the aramid fibre products as Teijin’s Twaron® and Technora® and DuPont's Kevlar®. The mechanical and physical properties of Twaron® and Kevlar® aramid fibres are not considerably different for analysis, according to the literature and handbooks [27].

Excessive cell disruption and tangling occurs due to calculations using the Lagrangian solution technique in ballistic impact simulation. Cells eroded only when severely distorted and compressive strength of cell was not effect the calculation. Inertia was preserved in the analysis by equally distributing the mass of the removed cells to the other nodes. The erosion logic based on an instantaneous geometric strain was assigned to the Twaron®/epoxy plates to prevent the calculation from terminating prematurely [10]. Erosion strain for orthotropic material models was typically between 1-2% of the instantaneous geometric strain [6, 13, 28]. The geometric strain was considered as 1.2 % for Twaron®/epoxy material and 2 % for lead and brass material in this study with removed cells mass taken into account [10-13, 29].

Table 2. Material properties of Kevlar129 used in the analysis [10-13].

| Material properties | | Strength/Elastic | |
|--|------------|---------------------------------|---------------|
| Reference density (g/cm ³) | 1.65 | Shear modulus (kPa) | 1.85701e6 |
| Orthotropic Engineering constants | | Failure\Material stress/Strain | |
| Young modulus 11(kPa) | 1.948e6 | Tensile failure stress 11 (kPa) | 1.2e6 |
| Young modulus 22(kPa) | 1.8e7 | Tensile failure stress 22 (kPa) | 1.85e6 |
| Young modulus 33(kPa) | 1.8e7 | Tensile failure stress 33 (kPa) | 1.85e6 |
| Poisson ratio 12 | 0.077551 | Maximum shear stress 12 (kPa) | 5.43e5 |
| Poisson ratio 23 | 0.062540 | Maximum shear stress 23 (kPa) | 7.7e04 |
| Poisson ratio 31 | 0.312031 | Maximum shear stress 31 (kPa) | 5.43e5 |
| Shear modulus 12(kPa) | 2.23e5 | Tensile failure strain 11 (kPa) | 0.02 |
| Shear modulus 23(kPa) | 1.85701e6 | Tensile failure strain 22 (kPa) | 0.060 |
| Shear modulus 31(kPa) | 2.23e05 | Tensile failure strain 33 (kPa) | 0.060 |
| Volumetric response | Polynomial | Maximum shear strain 12 | 1e20 |
| Bulk modulus-A1-T1 | 5.29e6 | Maximum shear strain 23 | 1e20 |
| Parameter A2 | 4e7 | Maximum shear strain 31 | 1e20 |
| Reference temperature (K) | 300 | Erosion/Geometric strain | Instantaneous |
| Specific heat (J/kg K) | 1.42e3 | Erosion strain | 1.2 |

3. RESULTS

3.1. Ballistic Test Results

Change of the thicknesses and the bullet initial/residual velocities with the number of layers were compared in Figure 5 (a) and (b), respectively. As expected, the thickness values of the plates increased with the number of layers. The ratio of average thickness to number of layers was between 0.26-0.28 mm. The impact velocity (initial velocity) of the bullet was measured between 380

m/s and 400 m/s with the first chronograph. During the ballistic tests, the initial velocity of the bullet differed slightly due to the change in the amount of gunpowder contained in the cartridge, so the standard deviation values of the bullet velocity were also given in Table 3. Average bullet initial/residual velocities, absorbed energy, specific energy absorption values as ballistic test results, areal density and the measured weights of the produced plates according to the number of layers were summarized (Table 3).

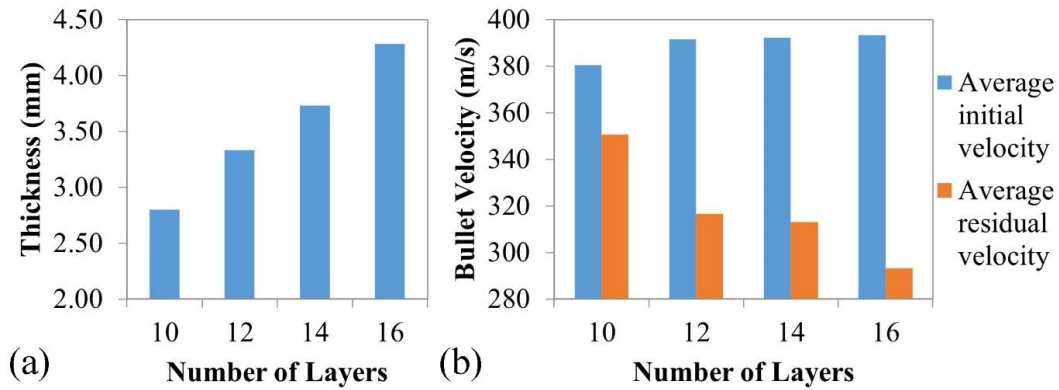


Figure 5. (a) Thickness of plates, (b) Average initial and residual bullet velocities

As a result of laminate containing more fibres, energy loss at impact increases with plate thickness. All the kinetic energy of the bullet was absorbed and stopped by the target at a ballistic limit velocity of 390 m/s for 18 layers through stretching the yarns, generating compressive waves along the thickness direction, deformation of the target, matrix cracking, fibre failure and delamination [6]. The absorbed energy increased with the increasing number of layers and reached 100% for the 18-layer sample by stopping the bullet. Therefore, the tests were determined for plates with 10-12-14-16 layers of aramid fabric and the residual velocities were compared with the data obtained using the finite element method. As seen from the deformation zones perforated by the bullet, the amount of fibre breakage on the back faces of the plates was found to increase with the increasing number of layers (Figure 6).

Depending on the initial velocity of the bullet before impact (V_i) and residual velocity after perforating the target (V_r), the initial, residual and absorbed energy values were calculated with the following analytical formulas.

$$\text{Initial (Impact) Energy (J), } E_i = 1/2mV_i^2 \quad (1)$$

$$\text{Residual energy of bullet after impact (J), } E_r = 1/2mV_r^2 \quad (2)$$

$$\text{Absorbed energy (J), } E_a = 1/2mV_i^2 - 1/2mV_r^2 \quad (3)$$

$$\text{Absorbed energy (\%), } E_a (\%) = (E_a / E_i) \times 100 \quad (4)$$

$$\text{Specific energy absorption (J/(gr/cm}^2\text{)), } E_s = E_a / (\text{Areal density}) \quad (5)$$

Table 3. Ballistic test results of Twaron®/epoxy plates

| Number of Layers | Plate Weight (g) | Average V_i (m/s)/SD | | Average V_r (m/s)/SD | | E_a (J) | E_a (%) | Areal Density (g/cm^2) | E_s ($J/(g/cm^2)$) |
|------------------|------------------|------------------------|------|------------------------|------|-----------|-----------|----------------------------|------------------------|
| | | | | | | | | | |
| 10 | 394.25 | 381 | 5.38 | 351 | 4.97 | 86.97 | 14.99 | 0.373 | 233.00 |
| 12 | 427.78 | 392 | 8.52 | 317 | 9.9 | 211.89 | 34.52 | 0.405 | 523.18 |
| 14 | 517.76 | 392 | 4.04 | 313 | 6.36 | 223.48 | 36.29 | 0.490 | 455.91 |
| 16 | 587.71 | 393 | 9.43 | 293 | 4.62 | 274.59 | 44.37 | 0.556 | 493.50 |
| 18 | 655.05 | 388 | 0.58 | - | - | 602.95 | 100.00 | 0.620 | 972.25 |

*SD: Standard deviation

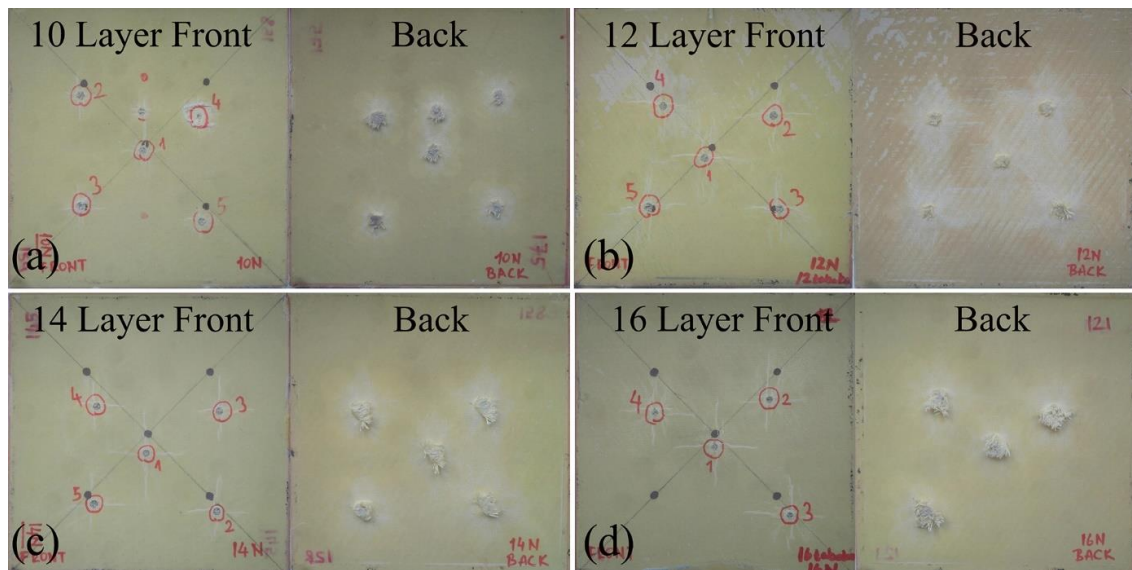


Figure 6. Back-face images of 10, 12, 14, 16 layer (a), (b), (c), (d) Twaron®/epoxy plates

3.2. Finite Element Model Results and Validation with Ballistic Tests

For each variable in the analysis, detailed time history results were obtained. Parameters such as bullet residual velocity, damage behaviour and bullet deformation over time were investigated. Compression of the target take place just below the bullet tip during ballistic impact, and the material begins to flow along the thickness direction as the bullet progresses. Bulge formation occur on the back face of the plate as a result of bullet compression following the target failure and finally the bullet and plug exit from the back face of the plate.

The Autodyn model can detect directional damage such as delamination with orthotropic failure criteria. Ballistic impact damage also depends on the shape of the 9 mm bullet. Near the impacted face shear plugging occurred, followed by a tensile fibre fracture region and delamination near the exit, both leads to bulk failure. Twaron®/epoxy fails, lost its load bearing capacity and the material properties change depending on the type of damage. Initiation of tensile damage for Twaron®/epoxy can be based on any combination of material stress and/or strain in orthotropic principal material directions. Friction, gravitational effects, angular velocity of the bullet are not taken into account in the simulations.

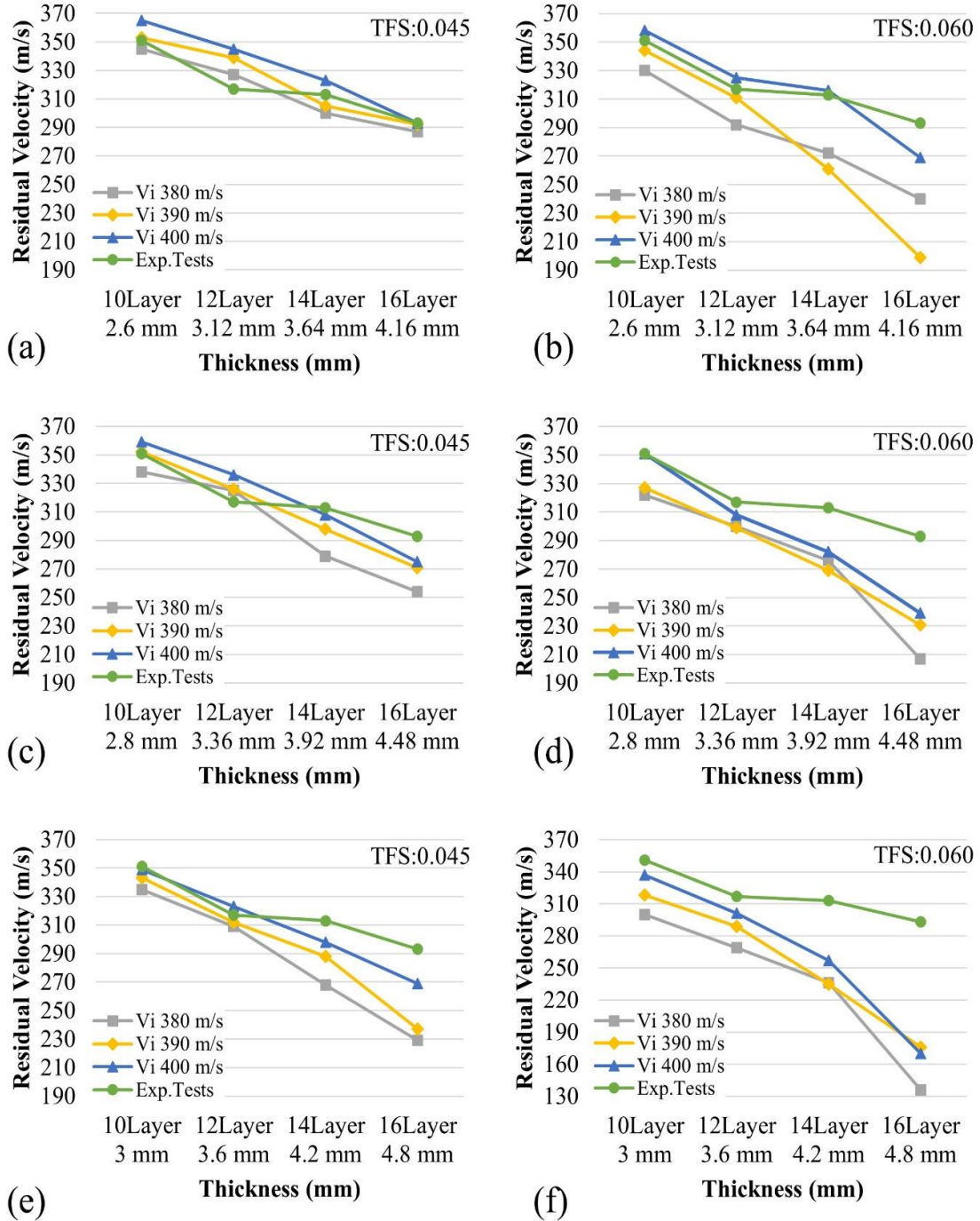


Figure 7. Residual velocities of (a) 0.26 mm/layer TFS:0.045, (b) 0.26 mm/layer TFS:0.060, (c) 0.28 mm/layer TFS:0.045, (d) 0.28 mm/layer TFS:0.060, (e) 0.30 mm/layer TFS:0.045, (f) 0.26 mm/layer TFS:0.060 at 0.06 ms

The residual velocities with the least errors closest to the experimental tests were obtained in the analysis with a layer thickness of 0.26 mm, a bullet initial velocity of 390 m/s, and TFS:0.045 (Figure 7 (a)). For 12 layers, the error in residual velocity was higher than the other layers. The measured residual velocity values for the 12- and 14-layer plates were found to be close in the experimental tests. The second closest residual velocity values to the experimental tests were 0.26 mm/layer, initial velocity: 400m/s, TFS:0.060 (Figure7(b)). The error in the residual velocity for 16 layer was higher than the other plates for this analysis. The residual velocity after perforation of the 16 layers was lower due to higher TFS:0.060 value causes the plate harder to perforate. The other closest residual velocity values for the parameters in Figure 7 (c) 0.28 mm/layer, initial velocity 390m/s, TFS:0.045 and in Figure 7 (e)

0.3mm/layer, initial velocity 400m/s TFS:0.045 were calculated in the analysis with higher error. It was observed that the error for residual velocity increase as the number of layers increases. The residual velocity error of the other analysis was higher when compared to experimental tests (Figure 7 (d) and (f)). It was found that the residual velocity increased with the increase in the impact velocity and there was a linear relationship between them.

After impact, the kinetic energy of the bullet was transferred and increases the energy of the plate and some of the kinetic energy was used for deformation of the bullet. During ballistic impact, the energy of the bullet was absorbed by the plate with different mechanisms, resulting in bullet retardation.

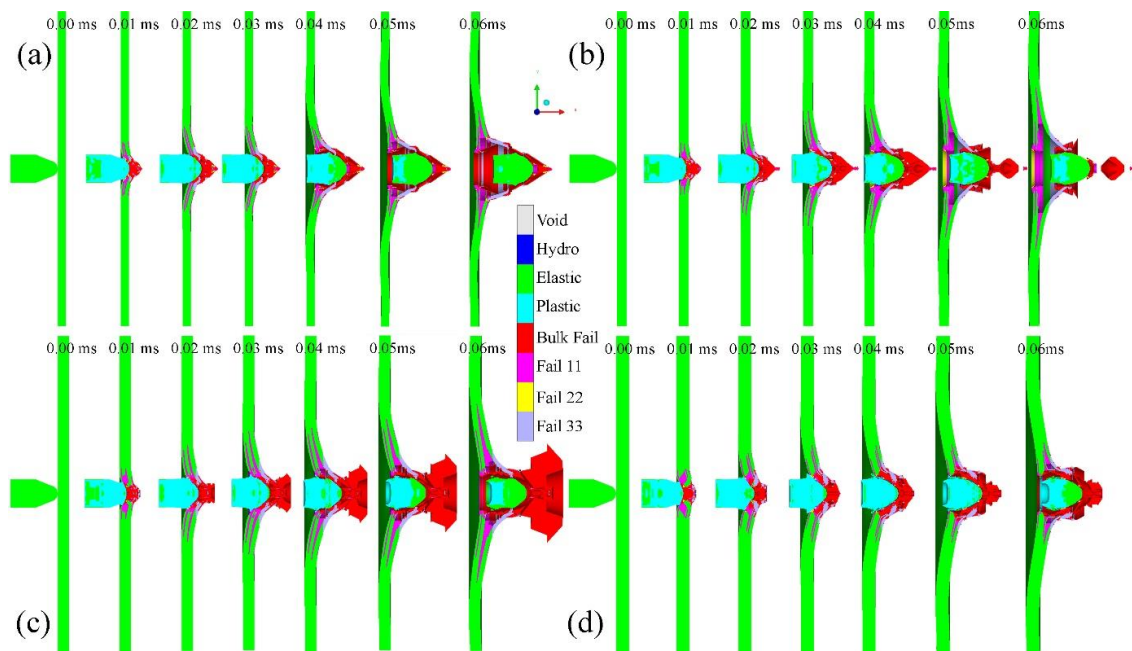


Figure 8. Perforation mechanisms, deformation, failure modes and failure directions of (a) 10 layer (2.6 mm), (b) 12 layer (3.12 mm), (c) 14 layer (3.64 mm), (d) 16 layer (4.16 mm) ($V_i=390\text{m/s}$, TFS:0.045) Twaron®/epoxy plates between 0.00 ms to 0.06 ms

In the analyses performed, the closest residual velocity results to the experimental study were obtained in Figure 8 (0.26mm/layer, $V_i=390\text{m/s}$, TFS:0.045) between 0.00-0.06 ms time range.

Perforation mechanisms, deformation, failure modes and failure directions of 10, 12, 14, 16 layer plates were shown in Figure 8 (a), (b), (c), (d) respectively. The perforation mechanisms observed

in the plates were due to delamination, fibre degradation and bulk failure. Delamination failure increased from 10 to 14 layers but decreased in 16 layers due to higher deflection of the plate by absorbing more kinetic energy of bullet.

As the number of layers increased, the contact duration of the bullet increased, causing retardation. As opposite, the decrease in the number of layers reduced the time required for the bullet to pass the thickness of the plate. The contact duration was determined by the travel of the bullet between 0.00 to 0.06 ms. When the bullet travels forward, the plate was damaged by different mechanisms and plug formation occurred in the plate as the major energy absorbing mechanism.

In Figure 9 (a), the energy percentages of the plate, bullet and work done were given. The plate and work done energy increased as the number of layers increased, while the bullet energy decreased with its speed. Work done represents the sum of the work done by constraints, work done by loads, work done by body forces, energy removed from

system by element erosion, work done by contact penalty forces. Current energy values were equal to the sum of internal, kinetic and hourglass energy of plate and bullet at 0.06 ms. During the penetration of the aramid layers, the bullet lost 13%, 16.7%, 25.84% and 28.49% of its energy at 0.06 ms for 10, 12, 14, and 16 layers, respectively. Most of this energy transferred to the plate and the rest was spent for work done.

The maximum diameter, length dimensions of the deformed bullet and front face hole diameter of plates were given in Figure 9 (b) (0.26 mm/layer, $V_i = 390\text{m/s}$, TFS:0.045). During the impact, the length of the bullet was shortened, cross-section was deformed into an ellipse and diameter increased compared to original (9 mm diameter, 15 mm length) dimensions. The bullet length increased slightly from 10 to 16 layers and the diameter decreased slightly from 10 to 14 layers, reached maximum value at 16 layers. This situation was defined as an increasing deflection of the plate in 16 layers with a rising bullet contact time and deformation.

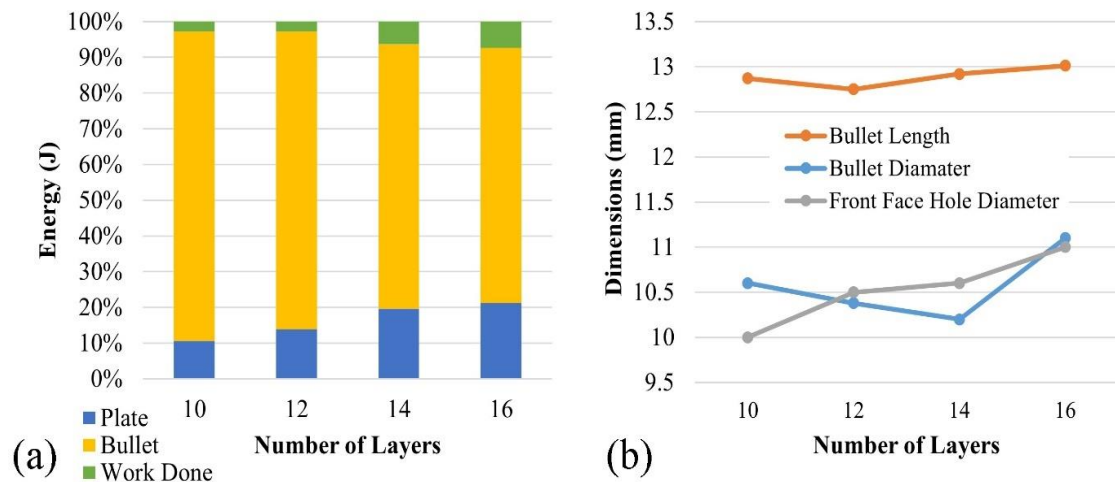


Figure 9. (a) Energy percent of plate, bullet and work done, (b) Deformed bullet dimensions and front face hole diameter of plates at 0.06 ms (0.26mm/layer, $V_i = 390\text{m/s}$, TFS:0.045)

4. CONCLUSION

The ballistic impact of a 9 mm FMJ RN bullet with different initial velocities on Twaron®/epoxy composite plates with various layer numbers and

thickness was investigated experimentally and numerically. The 9 mm bullet and Twaron®/epoxy plate was modelled axisymmetric in Autodyn-2D program for simplification and fast solution times of analysis.

- Based on the experimental and analysis results, Twaron®/epoxy plates with a layer number of 10-12-14-16 were completely perforated.
- 18 layers of Twaron®/epoxy armour was determined as the ballistic limit against the threat of 9 mm FMJ bullets with an average ballistic velocity of 390 m/s. Plates with 18 or more layers were absorbed all the energy of the bullet.
- It was stated that with the increase in the number of layers, the residual velocity values decreased as the perforation resistance of the plates increased, and it was far from the experimental data when the literature value of 0.06 for tensile failure strain 22 and 33 was used. Closer residual velocity results were obtained with the experimental tests by reducing the TFS value to 0.045.
- It was observed that with the increase in bullet impact velocity, the residual velocity also increases and there was a linear relationship between them.
- It was found that the optimum layer thickness was 0.26 mm for the best residual velocity values.
- The closest residual velocity analysis results to the experimental tests were obtained in the 0.26 mm/layer, $V_i = 390$ m/s, TFS: 0.045 at between 0.00-0.06 ms from three (0.26/0.28/0.30 mm) layer thicknesses and three (380/390/400 m/s) velocities.
- The work done energy for 16 layers was the highest compared to 10, 12, and 14 layers in (0.26 mm/layer, 390 m/s, TFS: 0.045) analysis. With the highest deflection of the plate and the increase in the contact time of the bullet in the plate, bullet reached the highest diameter, deformed in the form of an ellipse, and caused more local damage to the plate.
- As the number of layers increased, the plate and work done energy increased, while the bullet

energy decreased with its speed. The bullet lost minimum 13% and maximum 28.49% of its energy with full perforation at 0.06 ms (0.26 mm/layer, 390 m/s, TFS:0.045).

5. REFERENCES

1. Abrate, S., 2011. Impact Engineering of Composite Structures, 526, 403.
2. Vaidya, U.K., 2011. Impact Response of Laminated and Sandwich Composites. 526, CISM International Centre for Mechanical Sciences, 97-191.
3. Naik, N., Shirao, P., 2004. Composite Structures Under Ballistic Impact. Composite Structures, 66, 1-4, 579-590.
4. Zukas, J., 2004. Introduction to Hydrocodes. 49, Oxford, UK, 311.
5. Şenel, F., Balya, B., Parnas, L., 2004. İleri Kompozit Zırh Malzemelerin Balistik Analizi. Savunma Teknolojileri Kongresi, Ankara.
6. Bandaru, A. K., Vetiyatil, L., Ahmad, S., 2015. The Effect of Hybridization on The Ballistic Impact Behavior of Hybrid Composite Armors. Composites Part B: Engineering, 76, 300-319.
7. Bandaru, A. K., Ahmad, S., 2017. Ballistic Impact Behaviour of Thermoplastic Kevlar Composites: Parametric Studies. Procedia Engineering, 173, 355-362.
8. Wiśniewski, A., Pacek, D., 2010. Numerical Simulations of Penetration of 9 mm Parabellum Bullet into Kevlar Layers—Erosion Selection in AUTODYN Programme. Problemy Techniki Uzbrojenia, 39, 7-14.
9. Wiśniewski, A., Pacek, D., 2011. Numerical Simulations of Penetration of 9 mm Parabellum Bullet into Kevlar Layers: Erosion Selection in Autodyn Program. Problemy Mechatroniki: Uzbrojenie, Lotnictwo, Inżynieria Bezpieczeństwa, 2, 11-20.
10. Tham, C., Tan, V., Lee, H. P., 2008. Ballistic Impact of a KEVLAR® Helmet: Experiment and Simulations. International Journal of Impact Engineering, 35(5), 304-318.
11. Rajput, M.S., Bhuarya, M.K., Gupta, A., 2017. Finite Element Simulation of Impact on PASGT Army Helmet. Procedia Engineering, 173, 251-258.

12. Kumar, S., Gupta, D.S., Singh, I., Sharma, A., 2010. Behavior of Kevlar/epoxy Composite Plates Under Ballistic Impact. *Journal of Reinforced Plastics and Composites*, 29(13), 2048-2064.
13. Ansari, M.M., Chakrabarti, A., 2015. Effect of Bullet Shape and H/A Ratio on Ballistic Impact Behaviour of FRP Composite Plate: A Numerical Study. *International Journal of Research in Engineering and Technology*, 04(13), 2321-7308.
14. Soydan, A.M., Tunaboşlu, B., Elşabagh, A.G., Sarı, A.K., Akdeniz, R., 2018. Simulation and Experimental Tests of Ballistic Impact on Composite Laminate Armor, *Advances in Materials Science and Engineering*, 2018, 1-12.
15. Wiśniewski, A., Gmitrzuk, M., 2014. Validation of Numerical Model of the Twaron® CT709 Ballistic Fabric. *Problemy Mechatroniki: Uzbrojenie, Lotnictwo, Inżynieria Bezpieczeństwa*, 5, 19-31.
16. Gogineni, S., Gao, X.L., David, N., Zheng, J.Q., 2012. Ballistic Impact of Twaron CT709® Plain Weave Fabrics. *Mechanics of Advanced Materials and Structures*, 19(6), 441-452.
17. Dominiak, J., Stępień, Z., 2012. Finite-Element-Based Modeling of Ballistic Impact on a Human Torso Protected by Textile Body Armor. *Innovative Materials Technologies in Made-Up Textile Articles, Protective Clothing Footwear*, 2463, doi: <https://doi.org/10.13140/2.1.2463.1687>.
18. TEIJ Handbook Ballistics, 2019, (https://www.teijinaramid.com/wp-content/uploads/2019/11/TEIJ_Handbook_Ballistics_2019_DEF.pdf), Accessed on: 15.03.2022.
19. Köçük Taş, M., 2019. Tabakalı Kompozit Malzemelerin Balistik Zırh Özelliklerinin Geliştirilmesi. Yüksek Lisans, İnönü Üniversitesi Fen Bilimleri Enstitüsü, 72.
20. Datasheet for EPIKOTE™ Resin MGS™ LR160 Hexion Inc., (<https://www.hexion.com/CustomServices/PDFDownloader.aspx?type=tds&pid=83b88d44-5814-6fe3-ae8a-ff0300fcd525>), Accessed on: 15.03.2022.
21. Ballistic Resistant Protective Materials, 1985. US Department of Justice. National Institute of Justice Standard, N., NIJ-STD-0108.01.
22. Ramezani, A., Rothe, H., 2017. A New Approach to Modelling Fiber-Reinforced Plastics for Hydrocode Analysis. *SIMUL 2017: The Ninth International Conference on Advances in System Simulation*, Athens, Greece.
23. Sohn, S.W., Kim, H.J., Kim, Y.T., 2003. A Study on the High Velocity Impact Resistance of Hybrid Composite Materials. *Proceedings of the KSME Conference*, 273-278.
24. Özbek, Ö., 2021. Axial and Lateral Buckling Analysis of Kevlar/epoxy Fiber-reinforced Composite Laminates Incorporating Silica Nanoparticles. *Polymer Composites*, 42, 3, 1109-1122.
25. Gogineni, S., 2011. Finite Element Analysis of Ballistic Penetration of Plain Weave Twaron CT709® Fabrics: A Parametric Study. Master of Science, Texas A & M University, 146.
26. Cook W. H., 1983. A Constitutive Model and Data for Metals Subjected to Large Strains, High Strain Rates and High Temperatures. *Proceedings of the 7th International Symposium on Ballistics*. The Hague, Netherlands: International Ballistics Committee, 21, 541-547.
27. Beckwith, S.W., 2009. Composites Reinforcement Fibers: II-The Aramid and Polyethylene Families. *SAMPE Journal*, 45(6), 42-43.
28. AUTODYN, 1998. Theory Manual, Revision 4.0, Century Dynamics Inc.,
29. Lim, Y.Y., Miskon, A., Zaidi, A.M.A., Megat Ahmad, M.M.H., Abu Bakar, M., 2022. Numerical Simulation Study on Relationship between the Fracture Mechanisms and Residual Membrane Stresses of Metallic Material. *Journal of Functional Biomaterials*, 13(1), 20.

